GEOLOGICA CARPATHICA, JUNE 2019, 70, 3, 209–221 doi: 10.2478/geoca-2019-0012

Graptolite turnover and $\delta^{13}C_{org}$ excursion in the upper Wenlock shales (Silurian) of the Holy Cross Mountains (Poland)

SIGITAS RADZEVIČIUS[1,✉], PAWEŁ RACZYŃSKI[2], MARIUS UŽOMECKAS[1], AUDRIUS NORKUS[1] and ANDREJ SPIRIDONOV[1,3]

[1]Department of Geology and Mineralogy, Vilnius University, M.K. Čiurlionio 21/27, LT-03101, Vilnius, Lithuania; ✉sigitas.radzevicius@gf.vu.lt
[2]Institute of Geological Sciences, University of Wrocław, Pl. Maksa Borna 9, Wrocław 50-205, Poland
[3]Laboratory of Bedrock Geology, Nature Research Centre, Akademijos str. 2, LT-08412 Vilnius, Lithuania

(Manuscript received September 12, 2018; accepted in revised form March 25, 2019)

Abstract: The mid–late Homerian Age of the Silurian Period was a time of intense changes in biota, oceanic chemistry, and sea level and is known as the *lundgreni* extinction (for the graptolite extinctions), the Mulde bioevent (for the conodont turnover event) or the Homerian carbon isotope excursion (CIE) probably related to glacially influenced climate perturbation. New information on this interval from the deep water sedimentary and graptolite succession of the Kielce Region (Holy Cross Mountains, Poland) of the northern margin of the Małopolska Block is presented here based on analysis of the Prągowiec Ravine section. The *lundgreni–nilssoni* graptolite biozones interval have been recognized there. This interval is composed by dark shales with very rare benthic fauna, which indicate the deep open-marine (pelagic) paleoenvironment. Ten samples were taken for the $\delta^{13}C_{org}$ analysis from the *lundgreni* (2 samples), *parvus* (2 samples), *praedeubeli* (2 samples), *praedeubeli–deubeli* (1 sample), *ludensis* (2 samples) and *nilssoni* (1 sample) biozones. According to the $\delta^{13}C_{org}$ results, the first positive $\delta^{13}C_{org}$ excursion of the Mulde Bioevent is well recognized. The $\delta^{13}C_{org}$ values rise from −30.7 – −30.1 ‰ in the *lundgreni* Biozone to −29.3 – −28.7 ‰ in the *parvus* Biozone and fall below −30 ‰ in the *praedeubeli–deubeli* interval. The second positive $\delta^{13}C_{org}$ peak of the Mulde Event was not recognized in the Prągowiec Ravine. Based on the numerical comparisons using Raup-Crick metric of co-occurrences of graptolite species, the upper Homerian was characterized by significant between-biozone turnover of these taxa at the given locality.

Keywords: Poland, Holy Cross Mountains, Silurian, Mulde Event, geochemistry, $\delta^{13}C_{org}$.

Introduction

The Silurian was one of the most unstable periods in the Paleozoic, marked by significant environmental changes and biotic perturbations (Crampton et al. 2016). One such episode is in the late Wenlock Epoch (mid–late Homerian). Graptolite workers refer to the onset of this episode as the *lundgreni* extinction (Koren' 1987) or the "Große Krise" (Jaeger 1991), and conodont workers refer to the immediately preceding changes in conodont assemblages as the Mulde Event (e.g., Jeppsson et al. 1995) or Homerian carbon isotope excursion (CIE; Calner 2008). Although it is debatable whether the Mulde Event had a significant impact on conodont communities (e.g., Radzevičius et al. 2014c; Jarochowska et al. 2018), it has been determined that, at least in Baltica, the community structure and abundance fluctuation patterns radically changed as a consequence of the events (Spiridonov 2017; Spiridonov et al. 2017a). The impact on the microphytoplankton communities of the Mulde Event is not so clear and the changes in their taxonomic composition and the size distribution probably were more related to sea level changes (Porębska et al. 2004; Venckutė-Aleksienė et al. 2016; Spiridonov et al. 2017b). A twin-peaked positive carbon isotope excursion has been documented globally in the upper Wenlock. Such carbon isotope excursions of this age are documented: in Baltica (Samtleben et al. 1996; Wenzel & Joachimski 1996; Bickert et al. 1997; Kaljo et al. 1997, 1998, 2007; Samtleben et al. 2000; Porębska et al. 2004; Martma et al. 2005; Calner et al. 2006b, 2012; Jarochowska et al. 2014, 2016a, 2016b; Radzevičius et al. 2014c, 2016; Jarochowska & Munnecke 2016; Makhnach et al. 2018); Laurentia (Saltzman 2001; Noble et al. 2005; Cramer et al. 2006; Lenz et al. 2006; Sullivan et al. 2016); Avalonia (Corfield et al. 1992; Marshall et al. 2012; Blain et al. 2016; Fry et al. 2017); Timan (Shebolkin & Männik 2014); Perunica (Frýda & Frýdová 2014, 2016); and Gondwana (Vecoli et al. 2009). Thus, most of the stable carbon isotopic data are from the Baltica, Laurentia and Avalonia paleocontinents.

The purpose of the investigation is to document biostratigraphy, constrain the stable carbon isotopic trends of the middle–upper Homerian, and to enlighten the patterns of graptolite community change in the Kielce Region of the Holy Cross Mountains, Poland. Here we present the first stable carbon isotope ($\delta^{13}C_{org}$) data linked to a biostratigraphical framework

for the Kielce Region (the Małopolska Block), and the Homerian biogeochemical event in the deep water open marine facies environments.

Geological background

The Holy Cross Mountains (HCM) are located in central Poland (Fig. 1A) and expose Paleozoic rocks in the central part of the Teisseyre–Tornquist Zone (TTZ) which extends from the North Sea in the NW to the Black Sea in the SE. According to the differences in the stratigraphic, lithological, facies, and tectonic evolution of the Lower Paleozoic, the HCM are divided into the Łysogóry Region or Unit in the north (Fig. 1B) and the Kielce Region (part of Małopolska Block) in the south (Fig. 1B) (Dadlez et al. 1994).

The Łysogóry Unit is considered to be a passive margin of Baltica (Dadlez et al. 1994; Narkiewicz 2002). The Silurian succession of the Łysogóry Unit is without significant gaps (Modliński & Szymański 2001) and comprises lower Llandovery deep open-marine (pelagic) to uppermost Přídolí lagoonal/fluvial (continental) deposits (Kowalczewski et al. 1998; Kozłowski 2003). Most natural outcrops of Silurian strata are exposed in the "Silurian Zone" (Fig. 1B) of the Łysogóry Unit (Kozłowski 2008). The upper Ludlow positive carbon isotope excursion associated with the Lau Event was first documented from the "Silurian Zone" (Fig. 1B) of the Łysogóry Unit by Kozłowski & Munnecke (2010) but no data from the upper Wenlock were presented.

The Kielce Region is on the northern margin of the Małopolska Block (Fig. 1A). There are different opinions regarding the development of the Małopolska Block: (1) it has a peri-Gondwanan origin, rifted in the Cambrian and amalgamated with the margin of SW Baltica during the Cambrian–Early Ordovician (Bełka et al. 2002; Walczak & Belka 2017); and (2) the Małopolska Block originated near the present SW margin of Baltica (Cocks 2002; Nawrocki et al. 2007). However, the Kielce and the Łysogóry regions were paleogeographically separate sub-basins in the Silurian (Kozłowski 2008). The Łysogóry Region was located relatively distally and the Kielce Region more proximally in relation to the same orogen, in other words the Łysogóry Region was closer to Baltica then the Kielce Region (Kozłowski et al. 2004, 2014). The Silurian sequence in the Kielce Region has numerous stratigraphic gaps and is represented by lowermost Llandovery deep open-marine deposits through to upper Ludlow turbidites (Kozłowski & Tomczykowa 1999). Perhaps because of the dominance of clastic sedimentation, stable carbon isotopes have not been investigated in the Kielce Region.

The exposed upper Wenlock and Ludlow succession is about 600 m thick (Tomczyk 1962) and is divided into the upper Bardo, Prągowiec, and Niewachlów beds (Fig. 1C). The upper Bardo beds are dark yellow and brown clayey shales belonging to the *Cyrtograptus lundgreni* and probably *Pristiograptus parvus* (see below) graptolite biozones. The Prągowiec beds are composed of dark grey silty shale with rare limestone concretions and abundant graptolites from the *Gothograptus nassa* to *Saetograptus leintwardinensis* biozones (Tomczyk 1962). The Niewachlów beds are composed of medium-grained greywackes with mudstone interbeds (Malec 2001) with *Bohemograptus bohemicus* (Barrande), *B. bohemicus tenuis* (Bouček) (Tomczyk 1962) and trilobites of Ludfordian age (Tomczykowa 1993). The Bardo Diabase occurs between the Prągowiec and Niewachlów beds. Using ^{40}Ar–^{39}Ar isotope dating its age is either 424±6 Ma–415±2 Ma latest Ludlow and earliest Lochkovian (Nawrocki et al. 2013). The igneous intrusion is spatially separated from the sampled outcrops. Good preservation of organic skeletons of graptolites points to the absence of significant contact metamorphism in the studied part of the section.

Material and methods

About 50 samples from the upper Wenlock and lower Ludlow (*lundgreni–nilssoni* biozones) were collected from the Prągowiec Ravine (50°44'46.04" N, 21°01'46.77" E) located in the Kielce region (Małopolska Block) of the HCM (Fig. 1B) about 2 km north of Bardo village on the northern limb of the Bardo Syncline (Kozłowski et al. 2017).

Material for geochemical analysis has been selected from five small outcrops in the Prągowiec Ravine (Fig. 1C). The height of outcrops varies from 0.5 to 2 m. Ten samples with well-preserved graptolites were selected from the upper Bardo and the Prągowiec shales for stable carbon isotope analysis. Graptolites from these shales are important for precise biostratigraphy. Sampling at high-resolution (e.g., each 0.1 to 1 m) was not possible because the ravine is overgrown and is covered by recent mudflow deposits and anthropogenic debris and at the present is far away from H. Tomczyk's (1962) interpretation (Fig. 1C). Due to these factors and also to the complex folding and faulting of the shales, the exact superposition of layers below biozonal level is impossible to determine. Due to these severe constraints on the availability of the material, the resolution of carbon isotopic sampling in this study is kept approximately at two samples per biozone (see below), where biozones were determined based on abundant graptolite material. All the material is stored in the Geological Museum of Vilnius University, Lithuania.

Stable carbon isotope ($\delta^{13}C_{org}$)

Samples are mostly composed of terrigenous (shale) material with different carbonate content. For the purpose of the $\delta^{13}C_{org}$ analysis, the samples that were powdered were the same as those from which fossils were identified (total 10 samples). Approximately 0.9 mg of sample powder was used from each sample. Powder was dissolved using 5 N (mass equivalents) HCl acid for 24 hours at the room temperature to remove carbonate minerals. After that, the powder residue was washed with distilled water and dried.

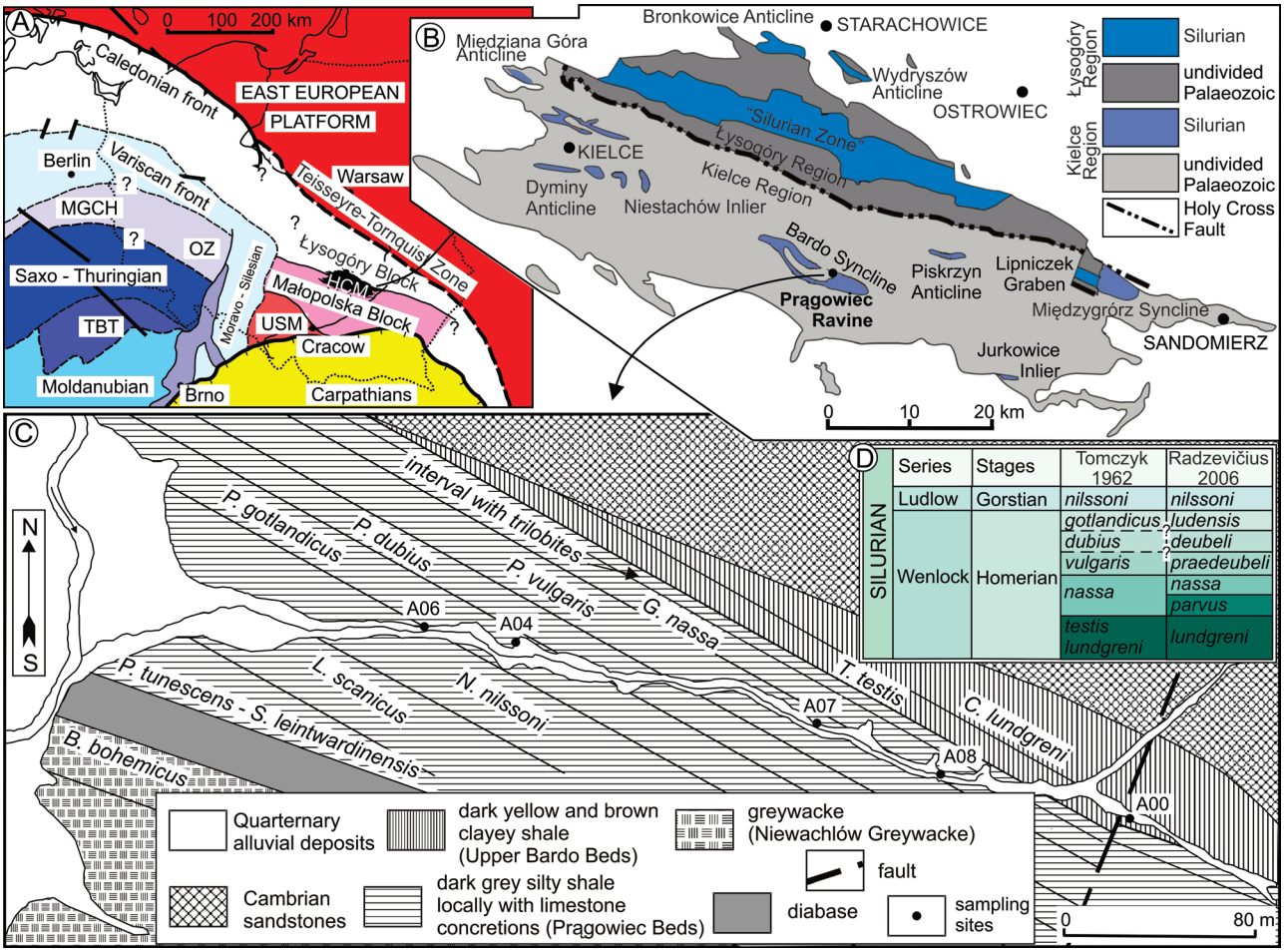

Fig. 1. A — Simplified structural map of Central Europe (Bełka et al. 2002). HCM — The Holy Cross Mountains; MGCH — Mid German Crystalline High; OZ — Odra Zone; TBT — Tepla–Barrandian Terrane; USM — Upper Silesian Massif. **B** — Distribution of Silurian rocks in the Holy Cross Mountains area (Kozłowski et al. 2014) and the Prągowiec Ravine location. **C** — stratigraphical interpretation of the Silurian succession in the Prągowiec Ravine (Tomczyk 1962, fig. 9). **D** — Possible correlation of the Prągowiec Ravine Upper Wenlock graptolite biozones (Tomczyk 1962) with those of revised Lithuanian (Radzevičius 2006).

After the pre-treatment removal of carbonates, all samples (at least two per sediment sample) were weighed and wrapped in tin capsules. The prepared samples were combusted with combustion module (Costech Analytical Technologies, Inc.) connected via Picarro Liaison Interface A0301 to the laser-based Picarro Cavity Ring-Down Spectrometer G2121-i. The stable carbon isotope ratio was measured in CO_2 and presented as per mil deviations from internationally accepted standards with the reproducibility of ±0.3‰ for $\delta^{13}C$. The international standards (IAEA-600, IAEA C1, IAEAC2 and SRM 4990C) were used for the calibration of the reference gas (CO_2).

Multivariate comparison of graptolite assemblages

In order to compare the compositional changes in graptolite assemblages in the Prągowiec Ravine, two methods were employed: non-metric multidimensional scaling and the comparison of turnover within the zones and among them. We employed a non-metric multidimensional scaling technique, a multivariate dimension reduction technique which is robust in revealing non-linear gradients in species composition (Patzkowsky & Holland 2012). We used the PAST program and the Raup-Crick metric (Hammer & Harper 2008), which is suitable for comparison of samples with differing and unknown abundances (Raup & Crick 1979). In our case, the latter property is especially desirable, since the abundance of graptolites is very difficult to measure, especially if there are variations in preservation (e.g., many fragmented rhabdosomes) and in the sizes of rock samples. In order to test the level of between-biozonal turnovers to inside-biozonal turnovers of graptolites in the Prągowiec Ravine, we performed all possible pair-wise comparisons between samples in a given biozone $c=(N_1^2-N_1)/2$, where N_1 is the number of samples in the first biozone) and between all the samples between two biozones $c=(N_1 \times N_2)$, where N_2 is the number of samples in the second biozone). For this purpose, as in the previous case, we used Raup-Crick compositional distance, which

was calculated in the *Vegan* package (Oksanen et al. 2018) for the R programming environment (R Development Core Team 2015). Later on, the yielded distributions of compositional distances were compared with each other using the non-parametric Mann-Whitney test.

The analysis was performed on the graptolite occurrence data from the *praedeubeli*, *deubeli* and *ludensis* biozones (spanning most of the upper Homerian), since only those biozones had more than two collected samples each and were represented by sufficiently abundant graptolite material. The *praedeubeli* Biozone was represented by 15 samples, the *deubeli* Biozone by 12 samples, and the *ludensis* Biozone by 18 unambiguously assigned samples with abundant graptolite material. The single occurrence of *Semigothograptus* cf. *meganassa* was not used in these multivariate analyses because of the ambiguity of its species assignment.

Graptolite biozones

H. Tomczyk (1962) distinguished the graptolite biozones in the Prągowiec Ravine (Fig. 1C), describing six graptolite biozones in the Homerian–lower Gorstian interval (Fig. 1D). Some of these biozones are not used at present. The Prągowiec Ravine graptolite revision and new graptolite biozones correlation of Tomczyk's biozones were given by E. Porębska (in Masiak 2010, fig. 20). At the same time as the above biozonations were being developed, S. Radzevičius (2006) distinguished graptolite assemblages and recommended the use of seven graptolite biozones (Fig. 1D) in the *lundgreni–nilssoni* interval of the Prągowiec ravine.

Cyrtograptus lundgreni Tullberg (Fig. 2A), *Monograptus flemingii* (Salter) (Fig. 2B); *Monoclimacis flumendosae* (Gortani) (Fig. 2C) and *Pristiograptus pseudodubius* Bouček occur in the Bardo beds (sample VU-U-10). *M. flemingii*, *Mcl. flumendosae* and *P. pseudodubius* are long ranging species, which appeared in the middle Sheinwoodian above the *riccartonensis* Biozone (Zalasiewicz et al. 2009) and disappeared in the middle Homerian during the *lundgreni* Event (Koren' 1987). *C. lundgreni* is the index species and its range defines the *lundgreni* Biozone (Zalasiewicz & Williams 1999).

The only *Testograptus testis* (Barrande) (Fig. 2D) identified was in the Bardo bed sample VU-U-6. A *testis* Biozone is recognized between the *lundgreni* and *nassa* biozones in the HCM (Tomczyk 1958; Ryka & Tomczyk 1959) as well in the Prągowiec ravine (Tomzcyk 1962). *T. testis* appeared later than *Cyr. lundgreni*, which accompanies *T. testis* until the *lundgreni* extinction. Therefore, the interval with *T. testis* represents the upper part of the *lundgreni* Biozone (Zalasiewicz et al. 2009) and is sometimes referred to it as the upper subzone (Jaeger 1991; Štorch 1994).

Pristiograptus parvus Ulst (Fig. 2E) and fragments of *Gothograptus nassa* (Holm) (Fig. 2F) occur in sample VU-U-7 which is composed of dark yellow clayey shales, probably of the Bardo beds. *G. nassa* ranges from the lower part of *parvus* Biozone to the middle part of the *praedeubeli* Biozone (Kozłowska et al. 2009) or the *parvus–nassa* interval (Maletz 2010). The short-ranging *P. parvus* appears after the *lundgreni* extinction and defines the *parvus* range Biozone (Ulst 1974).

Gothograptus nassa (Fig. 2H) and a trilobite pygidium of *Odontopleura* cf. *ovata* Emmrich (Fig. 2G) occur in Bardo beds sample VU-U-9. *G. nassa* ranges through the *parvus–praedeubeli* interval. A mass occurrence of benthic fauna (e.g., *Odontopleura*) marks the lower part of the *nassa* Biozone in the Prągowiec ravine (Tomczykowa 1957) and Bartoszyce IG 1 borehole (Porębska et al. 2004) in Poland. According to Calner et al.'s (2006a) data, *O. ovata* was recovered from just above the Grötlingbo Bentonite on Gotland. The Grötlingbo Bentonite is widespread in Laurussia at a stratigraphic level corresponding to the *parvus* Biozone (Kiipli et al. 2008).

Colonograptus praedeubeli (Jaeger) (Fig. 2K) and *G. nassa* (Fig. 2L) occur in the Prągowiec beds (sample VU-U-2). *C. praedeubeli* ranges from the *praedeubeli* Biozone to the middle of the *ludensis* Biozone (Koren' 1991), but is most common in the *praedeubeli* Biozone. *Col. praedeubeli* (Fig. 2M) also occurs in sample VU-U-8 (Prągowiec beds).

Colonograptus praedeubeli (Fig. 2O) occurs in sample VU-U-5 (Prągowiec beds). There is *Col.* cf. *deubeli* (Jaeger) (Fig. 2N) identified in the same sample. *Col. deubeli* is characterized by funnel- or trumpet-like sicula with distinct dorsal process and rapid increase in rhabdosome width (Koren' & Suyarkova 1994). Our *Col.* cf. *deubeli* specimen has a moderately expanded sicular aperture, but the width of rhabdosome increases gradually. *Col.* cf. *deubeli* is similar in terms of rhabdosome width to *Pristiograptus idoneus* Koren', but differs in the form of the sicula. The sicula of *P. idoneus* is strongly ventrally curved (Koren' 1992). Some fragments of retiolitids with the *nassa* type of apertural hoods have been found in the same sample (Fig. 2P). There is *G. nassa*, *Semigothograptus meganassa* (Rickards & Palmer 2002) and *Neogothograptus eximinassa* Maletz with genicular hoods of the *nassa* type in the *parvus–ludensis* interval (Kozłowska 2016). The flattened and poor preservation specimens complicate identification. Retiolitids are distinguished based mostly on isolated, 3D material (Lenz & Kozłowska 2007). However, *N. eximinassa* marks the *ludensis* Biozone (Maletz 2008), *S. meganassa* and *G. nassa* have similar stratigraphic ranges, and are confined to the *parvus–deubeli* interval (Kozłowska et al. 2009; Kozłowska 2016). The main difference that can be distinguished in the poorly preserved material between *S. meganassa* and *G. nassa* is in the width of rhabdosome. *S. meganassa* is wider than *G. nassa* (Kozłowska-Dawidziuk et al. 2001; Rickards & Palmer 2002) and *N. eximinassa* as well. Our specimen is relatively wide (approximately 2 mm) but the structure of apertural hoods is invisible and the proximal end of rhabdosome is absent. Based on this, this specimen has been identified as *Semigothograptus* cf. *meganassa*. However, the index species *Col. deubeli*, the first appearance of which marks the base of the *deubeli* and ranges to the middle of the *ludensis* Biozone (Jaeger 1991; Koren' 1991), is not found in the sample. Therefore, the graptolite assemblage of VU-U-5 sample is interpreted as belonging to the *praedeubeli–deubeli* interval.

Pristiograptus virbalensis Paškevičius and *Col. ludensis* (Murchison) (Fig. 2J) occur in sample VU- U-3 (Prągowiec beds). *P. virbalensis* is known from the *praedeubeli–nilssoni* biozones in Lithuania (Radzevičius et al. 2014a). *Col. ludensis* is the index species for the uppermost Homerian *ludensis* Biozone (Zalasiewicz et al. 2009).

P. frequens Jaekel and *Col. gerhardi* (Kühne) (Fig. 2I) occur in sample VU-U-1 (Prągowiec beds). The long-ranging

Fig. 2. The main fauna from the Prągowiec Ravine. **A–C:** Sample VU-U-10, upper Bardo beds, *lundgreni* Biozone; A — *Cyrtograptus lundgreni* Tullberg, SV-PER-027; B — *Monograptus flemingii* (Salter), SV-PER-026; C — *Monoclimacis flumendosae* (Gortani), SV-PER-026a. **D** – Sample VU-U-6, upper Bardo beds, *lundgreni* Biozone, *Testograptus testis* (Barrande), SV-PER-018. **E, F:** Sample VU-U-7, upper Bardo beds, *parvus* Biozone; E — *Pristiograptus parvus* Ulst, SV-PER-023; F — *Gothograptus nassa* (Holm), SV-PER-023a. **G, H:** Sample VU-U-9, upper Bardo beds, *parvus* Biozone; G — trilobite pygidium of *Odontopleura* cf. *ovata* Emmrich SV-PER-001a; H — *Gothograptus nassa* (Holm) SV-PER-001. **I** — Sample VU-U-1, Prągowiec beds, *ludensis* Biozone, *Colonograptus gerhardi* (Kühne) SV-06-8. **J** — Sample VU-U-3, Prągowiec beds, *ludensis* Biozone, *Colonograptus ludensis* (Murchison) SV-A04-2. **K, L:** Sample VU-U-2, Prągowiec beds, *praedeubeli* Biozone; K — *Colonograptus praedeubeli* (Jaeger) SV-69-6; L — *Gothograptus nassa* (Holm) SV-69-9. **M** — Sample VU-U-8, Prągowiec beds, *praedeubeli* Biozone, *Colonograptus praedeubeli* (Jaeger) SV-A04-6. **N–P:** Sample VU-U-5, Prągowiec beds, *praedeubeli–deubeli* biozones; N — *Colonograptus* cf. *deubeli* (Jaeger) SV-A07-1; O — *Colonograptus praedeubeli* (Jaeger) SV-A07-1a; P — *Semigothograptus* cf. *meganassa* (Rickards Palmer) SV-A07-1b. **R** — Sample VU-U-4, Prągowiec beds, *nilssoni* Biozone, *Neodiversograptus nilssoni* (Barrande) SV-A06-4. Scale bars are 1mm.

P. frequens appears in the *nassa* Biozone and disappears in the *leintwardinensis* Biozone (Urbanek et al. 2012) or above the *tenuis* Biozone (Štorch et al. 2014). *Col. gerhardi* appears in the upper part of the *ludensis* Biozone and disappears in the lower part of the *nilssoni* Biozone (Kozłowska-Dawidziuk et al. 2001; Radzevičius & Paškevičius 2005) but dominated in the upper part of the *ludensis* Biozone (Štorch et al. 2016).

An approximately 10 cm long mesial rhabdosome fragment of *Neodiversograptus nilssoni* (Barrande) (Fig. 2R) was found in the sample VU-U-4 (Prągowiec beds). *N. nilssoni* indicates the lower part of the Ludlow and is the index species for the *nilssoni* Biozone (Zalasiewicz et al. 2009).

In summary, the samples for the $\delta^{13}C_{org}$ analyses come from *lundgreni*, *parvus*, *praedeubeli–deubeli*, *ludensis* and *nilssoni* biozones (Table 1). There are no findings of typical *Col. Deubeli,* the index species of the *deubeli* Biozone, in the studied isotopic samples. Graptolites described in the samples VU-U-2, VU-U-8 and VUU-5 have long range and can be discovering in both *praedeubeli*, *deubeli* biozones. According to that, the *praedeubeli–deubeli* interval is not split into the separate biozones there.

Results and discussion

Turnover in graptolite assemblages

Although some indications of the community turnover can be distinguished from the range charts of the graptolite species, the ecological significance of those changes is not especially obvious. The composition of ecological communities is expressed as the identity of species and their abundance. Therefore, even if we observe a very similar set of species in two consecutive zones, if the relative frequencies of species in these zones are very different the final compositions in these two zones will be very ecologically different. As a result, numerical comparisons of sets of assemblages between zones can be used in statistical testing of significance of temporal changes. If the turnover between zones is continuous (when compositions change continuously without breaks), we should expect the fossil assemblages to significantly overlap in the multivariate compositional spaces. On the other hand if there are sharp changes in assemblage composition between zones we should expect clear separation.

The comparison of distances between samples in the *praedeubeli* Biozone Median=0.21, SD=0.21 with distances between samples of *praedeubeli* and *deubeli* biozones Median=0.658, SD=0.21 revealed their highly significant difference, $p<0.01$ (Fig. 3A). Similarly, there is a highly significant difference between sample distances in the *deubeli* Biozone Median=0.211, SD=0.16 and between distribution of distances between samples from the *deubeli* and *ludensis* biozones Median=0.817, SD=0.11, $p<0.01$ (Fig. 3B). A similar pattern of divergence can be seen between assemblage distances in the *ludensis* Biozone Median=0.249, SD=0.27, and the assemblage compositional distances between *deubeli* and *ludensis* biozones, Median=0.817, SD=0.11, $p<0.01$ (Fig. 3C). Although an overlap in distances can be observed between consecutive biozones, there is strong separation between assemblages. Moreover, compositional distances between biozones show strong modality, which points to the conclusion that biozonal boundaries represent genuine turnover episodes in development of graptolite faunas in the area represented by samples from the Prągowiec Ravine. Additionally, it appears that the differences in graptolite assemblages were on average greater between the *deubeli* and *ludensis* biozones (difference between medians of distances=0.448) than between the *praedeubeli* and *deubeli* biozones (difference between medians of distances=0.547).

The same conclusion of between-zonal differentiations in graptolite assemblages can be drawn based on the results of the non-metric multidimensional scaling analysis of the composition of graptolite assemblages (Fig. 4). The assemblages from all three analysed biozones are very clearly distinguished, with graptolite communities from the *praedeubeli* and *deubeli* biozones being more closely related to each other, as was suggested by the results of the previously presented pair-wise comparative analyses. Based on the taxonomic compilation of

Table 1: Isotopic data for the Prągowiec Ravine samples.

	Sample No.	Sampling sites	GPS coordinates	Formation	Biozone	$\delta^{13}C_{org}$	Fauna
1	VU-U-10	A00	50°44'46.2" N, 21°02'16.0" E	Bardo beds	*lundgreni*	−30.7	*M. flemingii, Mcl. flumendosae, P. pseudodubius, Cyr. lundgreni*
2	VU-U-6	A00	50°44'46.2" N, 21°02'16.0" E	Bardo beds	*lundgreni*	−30.1	*T. testis*
3	VU-U-7	A00	50°44'46.2" N, 21°02'16.0" E	Bardo beds	*parvus*	−29.3	*P. parvus, G. nassa*
4	VU-U-9	A00	50°44'46.2" N, 21°02'16.0" E	Bardo beds	*parvus*	−28.7	*G. nassa*, *Odontopleura* cf. *ovata*
5	VU-U-2	A08	50°44'46.8" N, 21°02'10.8" E	Prągowiec beds	*praedeubeli*	−30.2	*Col. praedeubeli, G. nassa*
6	VU-U-8	A04	50°44'48.7" N, 21°02'01.9" E	Prągowiec beds	*praedeubeli*	−30.8	*Col. praedeubeli*
7	VU-U-5	A07	50°44'47.6" N, 21°02'08.1" E	Prągowiec beds	*praedeubeli–deubeli*	−30.4	*Col. praedeubeli, Col.* cf. *deubeli, S.* cf. *meganassa*
8	VU-U-3	A04	50°44'48.7" N, 21°02'01.9" E	Prągowiec beds	*ludensis*	−31.2	*P. virbalensis, Col. ludensis*
9	VU-U-1	A06	50°44'49.3" N, 21°01'58.1" E	Prągowiec beds	*ludensis*	−30.2	*P. frequens, Col. gerhardi*
10	VU-U-4	A06	50°44'49.3" N, 21°01'58.1" E	Prągowiec beds	*nilssoni*	−30.5	*N. nilssoni*

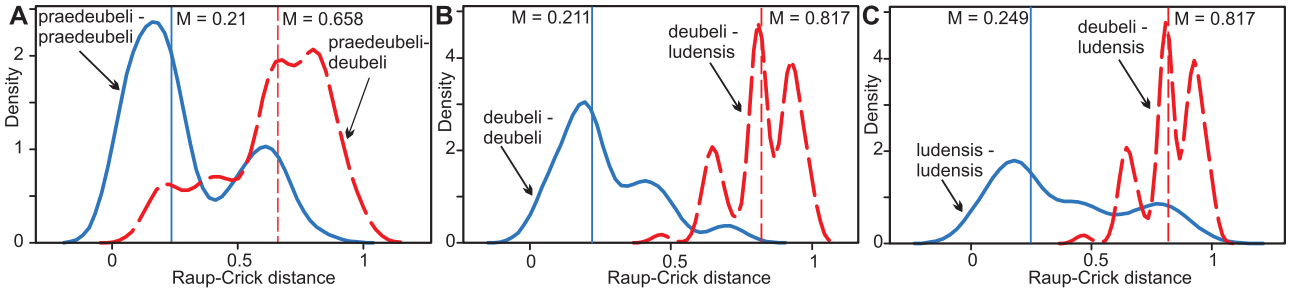

Fig. 3. Raup-Crick distances of graptolite assemblages from the Prągowiec Ravine (p-values show probabilities of null hypothesis for equality of medians): **A** — between samples of the praedeubeli Biozone (c=105), and between samples of the praedeubeli and deubeli (c=180) biozones ($p<0.01$); **B** — between samples of the deubeli Biozone (c=66), and between samples of the deubeli and ludensis (c=216) biozones ($p<0.01$); **C** — between samples of the ludensis Biozone (c=153), and between samples of the deubeli and ludensis (c=216) biozones ($p<0.01$). Arrows point to the medians for each distribution of between sample distances. Here c=the number of pairwise comparisons in each category.

Koren' (1991), the *ludensis* Biozone witnessed significant restructuring in diversity of graptolites–retiolitids increased in species richness and monograptids a decline in species richness. Similarly, in the Canadian sections described by Lenz (1994, 1995), there was a significant turnover of monograptids between the *deubeli* and *ludensis* biozones. According to the global sequencing of the graptoloid clade, the *ludensis* Biozone marked an interval of significant increase in graptolite diversity which ended in the early Ludlow (Cooper et al. 2014). At least two large extinction events separated by hundreds of thousands of years occurred in the late Homerian, not including the *lundgreni* extinction event (Crampton et al. 2016). Thus the intensive graptolite turnover described in the Prągowiec Ravine is part of the wider pattern.

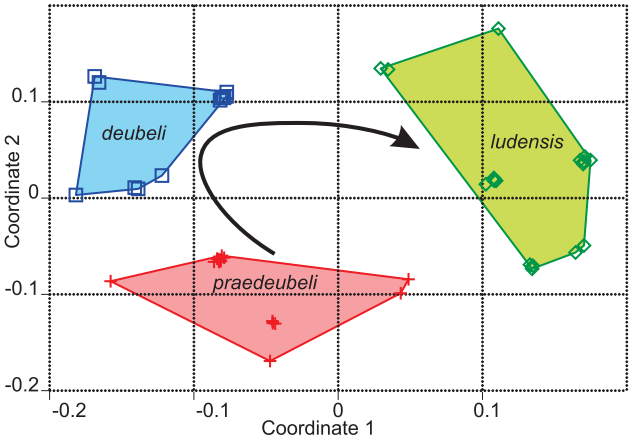

Fig. 4. Non-metric multidimensional scaling of graptolite assemblages from the Prągowiec Ravine (Stress=0.26).

Trend in $\delta^{13}C_{org}$ values

The $\delta^{13}C_{org}$ values are low and vary from −31.2 ‰ to −28.7 ‰; (Table 1). Similar variations in upper Homerian $\delta^{13}C_{org}$ values are recorded from the part of Poland corresponding to the West of Baltica (Porębska et al. 2004; Sullivan et al. 2018). The highest variation of $\delta^{13}C_{org}$ values is found in the upper Bardo beds. The values rise from −30.7 ‰ and −30.1 ‰ in the *lundgreni* Biozone to −29.3–28.7 ‰ in the *parvus* Biozone (Fig. 5) and drop in the Prągowiec beds and fluctuate overall by 1 ‰ between −31.2 ‰ and −30.2 ‰ through the *praedeubeli – nilssoni* Biozone interval (Fig. 5).

There are two positive $\delta^{13}C_{carb}$ peaks in the mid-upper Homerian (Cramer et al. 2011; Melchin et al. 2012). The first $\delta^{13}C_{carb}$ peak is found in the *parvus–nassa* biozones and second one in the *ludensis* Biozone. Such interpretation is based on material from the West Midlands (England) and Gotland (Cramer et al. 2012). The West Midlands sections are dominated by shallow marine facies with very rare graptolites and the correlation of these localities is based only on conodont biostratigraphy, sequence stratigraphy and high-precision zircon (U–Pb) dating of bentonites. Therefore, bearing in mind all the possible uncertainties in correlation, the incorporation of $\delta^{13}C_{carb}$ excursion with graptolite biozones should be imprecise. In the material from the Viduklė–61 borehole (Lithuania) with a continuous graptolite sequence, the first positive excursion represents the *parvus* Biozone to lower *praedeubeli* Biozone interval and the second positive excursion represents the *deubeli* Biozone to lower *ludensis* Biozone (Radzevičius et al. 2014a) for the Gėluva Regional Stage in Lithuania (Fig. 5). After graptolite revision from the West Midlands, the same conclusions have been reached by Fry et al (2017).

In the gamma log data from the Viduklė–61 well, two cycles of ~16.7 m and five with ~6.7 m period lengths were determined in the Gėluva interval (Fig. 5) (Radzevičius et al. 2014b). Similar cyclicities were found in other mid-upper Homerian geological sections of West Lithuania (Radzevičius et al. 2017). The Gėluva age corresponds to the mid-later Homerian, namely from 428.45±0.35 Ma to 427.86±0.32 Ma (total ~0.59 Ma) (Cramer et al. 2015). Based on these dates, long cycles are about 0.3 Ma and short about 0.12 Ma. The duration of cycles alone could be tentatively interpreted as the 4th and 5th order cycles which are close to the Milankovitch eccentricity cycles generated by the orbital forcing (Miall 2010).

Two stage slices (Ho2 and Ho3) have been distinguished in the mid-upper Homerian (Cramer et al. 2011) or the Gėluva

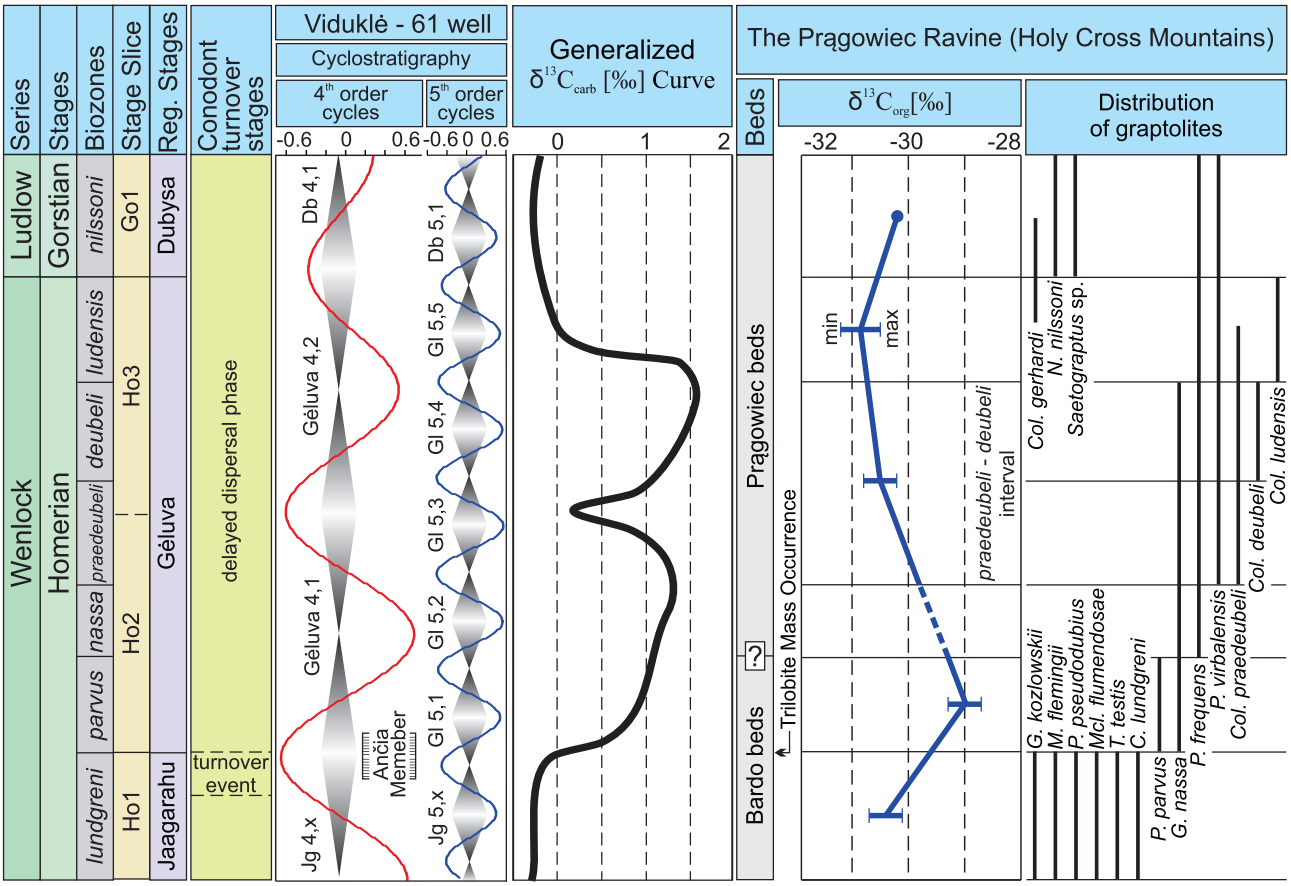

Fig. 5. Mid–upper Homerian global stratigraphical scale (Melchin et al. 2012); graptolite biozones (Koren' et al. 1996); stage slices (Cramer et al. 2011); regional stages of the East Baltic (Paškevičius et al. 1994); Conodont turnover stages (Radzevičius et al. 2016); cyclostratigraphy in the Viduklė-61 borehole and situation of the Ančia Member (Radzevičius et al. 2017); generalized $\delta^{13}C_{carb}$ curve (Cramer et al. 2011); lithology (Tomczyk 1962); $\delta^{13}C_{org}$ data (this paper) and generalized distribution of graptolites (Radzevičius 2006) of the Prągowiec Ravine (HCM, Poland).

Regional Stage in Lithuania. A stage slice is an informal stratigraphic unit that is defined on the basis of biochemostratigraphy. According to Cramer et al. (2011), the base of the Ho2 slice lies within the *parvus* Biozone and includes the first peak of the Mulde $\delta^{13}C$ excursion. The Ho3 slice ranges from the base of the *ludensis* Biozone to the base of the *nilssoni* Biozone with the second peak of the Mulde $\delta^{13}C$ excursion. *P. parvus* are found from the upper Bardo Beds in the Prągowiec Ravine. According to that, the lower Ho2 slice boundary doesn't directly corresponding to the Bardo and Prągowiec beds boundary. In the cyclostratigraphic data from West Lithuania (Radzevičius et al. 2017), the boundary between Ho2 and Ho3 is coincident with the boundary between Gėluva 4,1 and Gėluva 4,2 (4^{th} order) sedimentary cycles.

It has previously been hypothesized that the evolutionary turnover of conodonts was spread through the upper Homerian (Jeppsson et al. 1995), although more detailed integrated analysis of interregional data revealed that the first appearances of zonal taxa, *O. bohemica longa*, *K. ortus absidata* and *Ctenognathodus murchisoni* converge to the beginning of the Mulde event as indicated by the integrated stratigraphy (Radzevičius et al. 2016). Therefore appearances of those taxa in different regions should be highly diachronous (see in fig. 5 "delayed dispersal phase model", which shows an initial phase of evolutionary changes which is followed by the longer dispersal phase of conodont taxa). On the other hand, based on the analyses of local communities, it was shown that there was no significant community turnover in conodonts at the proposed boundary of the Mulde event (Jarochowska et al. 2018). Since there is positive evidence on evolutionary taxic disappearance and appearance (Jeppsson et al. 1995; Radzevičius et al. 2016), this lack of congruence could be explained by disproportionate effects of the Mulde turnover event on rare taxa. On the other hand, although the composition was similar in conodonts before and after the Mulde event, their communities changed to a more even and simple abundance distribution, and there was a shift to lower abundance and higher autocorrelation of abundance fluctuations which points to the transition to differing community states in the upper Homerian in the conodont clade (Spiridonov 2017; Spiridonov et al. 2017a).

On the other hand, range data for graptolites (including those presented here) and the multivariate analyses of their cooccurrences point to the possibility that the late Homerian

experienced several significant turnover events between biozones. Those are possibly related to the periodic sea level perturbations associated with the 4th and 5th order cycles which were clearly distinguished in the Baltic data (Fig. 5, and also Radzevičius et al. 2017) and briefly described in this paper. The same physical changes in environment are highly congruent with Cramer et al.'s (2011) proposed stage slices of the Homerian which are conceptually similar to assemblage biozones (Fig. 5). Moreover, recent cyclostratigraphic–spectral analytical studies revealed that external forcing due to Milankovitch forcing was a significant factor in driving changes in community compositions, and abundance of conodonts (Spiridonov et al. 2016, 2017a), as well as macroevolutionary diversity of graptolites during the Ordovician and Silurian (Crampton et al. 2018). The confluence of evidence points toward the dominance of the "common geological cause" (sensu Peters & Foote 2002) mechanisms of change in stratigraphy, ecology and macroevolution of biota in the Silurian.

The first $\delta^{13}C_{org}$ excursion is well represented in the *parvus* Biozone in the Prągowiec Ravine and related to the trilobite mass occurrence interval in the upper part of the Bardo beds (Fig. 5). This interval could be correlated with upper part of microlaminated, varve-like marlstone of the Ančia Member in the Lithuania (Radzevičius et al. 2014a) and with the lower part of Ho2. The second $\delta^{13}C_{org}$ excursion is very indistinct. This could be related to the deep marine facies which dominate the sedimentary record at the Prągowiec Ravine. A similar situation is found in the Zwierzyniec-1 borehole from deep marine facies of South-East Poland (Sullivan et al. 2018). The magnitudes of $\delta^{13}C$ excursions are higher in shallow water than in deeper water settings (Noble et al. 2005), which makes it more difficult to distinguish them in offshore shales. On the other hand, it can be related to low sampling resolution. However, the present results are consistent with previous observations and show that the $\delta^{13}C_{org}$ data can be used as a supporting data for stratigraphic correlation even in terrigenous deep water facies.

Conclusions

The first positive Homerian $\delta^{13}C_{org}$ excursion peak is well represented in the Prągowiec Ravine and is in the *parvus* Biozone (upper part of Bardo beds). The upper Bardo beds can be correlated with the lower part of the Ho2 stage slice and the Ančia Member in the Baltic Silurian Basin as well. Nevertheless, the $\delta^{13}C_{org}$ curve shows a broadly similar trend to that represented in the global Homerian $\delta^{13}C_{carb}$ curve and can be used for the correlation between these datasets.

Additionally, the quantitative analyses of graptolite samples revealed that there was a significant turnover in this planktic group between biozones in the late Homerian *(post lundgreni* Event*)* at the studied site. The greatest turnover occurred between the *deubeli* and *ludensis* biozones in the Prągowiec Ravine area.

Acknowledgements: We thank colleagues J. Mažeika and R. Paškauskas from the Nature Research Centre (Lithuania) for undertaking isotope analyses. We sincerely thank M. Whittingham for the English correction A.S.'s research is supported by the Research Council of Lithuania grant No. 09.3.3-LMT-K-712-02-0036. This research was supported by the Open Access to research infrastructure of the Nature Research Centre under the Lithuanian open access network initiative. This is a contribution to "IGCP 652: Reading geological time in Paleozoic sedimentary rocks: the need for an integrated stratigraphy" and to "Event Stratigraphy in the Silurian Sedimentary Basin of Lithuania", a Vilnius University project.

References

Bełka Z., Valverde-Vaquero P., Dörr W., Ahrendt H., Wemmer K., Franke W. & Schäfer J. 2002: Accretion of first Gondwana-derived terranes at the margin of Baltica. In: Winchester J.A., Pharaoh T.C. & Verniers J. (Eds.): Palaeozoic amalgamation of Central Europe. *Geol. Soc. London, Spec. Publ.* 201, 19–36.

Bickert T., Pätzold J., Samtleben C. & Munnecke A. 1997: Paleoenvironmental changes in the Silurian indicated by stable isotopes in brachiopod shells from Gotland, Sweden. *Geochim. Cosmochim. Acta* 61, 2717–2730.

Blain J.A., Ray D.C. & Wheeley J.R. 2016: Carbon isotope ($\delta^{13}C_{carb}$) and facies variability at the Wenlock–Ludlow boundary (Silurian) of the Midland Platform, UK. *Can. J. Earth Sci.* 53, 725–730.

Calner M. 2008: Silurian global events — at the tipping point of climate change. In: Elewa A.M.T. (Ed.): Mass extinctions. *Springer Verlag*, Berlin, 21–57.

Calner M., Ahlberg P., Axheimer N. & Gustavsson L. 2006a: The first record of *Odontopleura ovata* (Trilobita) from Scandinavia: Part of a middle Silurian intercontinental shelly benthos mass occurrence. *GFF* 128, 33–37.

Calner M., Kozłowska A., Masiak M. & Schmitz B. 2006b: A shoreline to deep basin correlation chart for the middle Silurian coupled extinctionstable isotopic event. *GFF* 128, 79–84.

Calner M., Lehnert O. & Jeppsson L. 2012: New chemostratigraphic data through the Mulde Event interval (Silurian, Wenlock), Gotland, Sweden. *GFF* 134, 65–67.

Cocks L.R.M. 2002: Key Lower Palaeozoic faunas from near the Trans-European Suture Zone. Winchester J.A., Pharaoh T.C. & Verniers J. (Eds.): Palaeozoic amalgamation of Central Europe. *Geol. Soc. London, Spec. Publ.* 201, 37–46.

Cooper R.A., Sadler P.M., Munnecke A. & Crampton J.S. 2014: Graptoloid evolutionary rates track Ordovician–Silurian global climate change. *Geol. Mag.* 151, 349–364.

Corfield R.M., Siveter D.J., Cartlidge J.E. & McKerrow W.S. 1992: Carbon isotope excursion near the Wenlock–Ludlow, (Silurian) boundary in the Anglo–Welsh area. *Geology* 20, 371–374.

Cramer B.D., Kleffner M.A. & Saltzman M.R. 2006: The Late Wenlock Mulde positive carbon isotope excursion in North America. *GFF* 128, 85–90.

Cramer B.D., Brett C.E., Melchin M.J., Männik P., Kleffner M.A., McLaughlin P.I., Loydell D.K., Munnecke A., Jeppsson L., Corradini C., Brunton F.R. & Saltzman M.R. 2011: Revised correlation of Silurian Provincial Series of North America with global and regional chronostratigraphic units and $\delta^{13}C_{carb}$ chemostratigraphy. *Lethaia* 44, 185–202.

Cramer B.D., Condon D.J., Söderlund U., Marshall C., Worton G.J., Thomas A.T., Calner M., Ray D.C., Perrier V., Boomer I., Patchett P.J. & Jeppsson L. 2012: U–Pb (zircon) age constraints on the timing and duration of Wenlock (Silurian) paleocommunity collapse and recovery during the 'Big Crisis'. *Bull. Geol. Soc. Am.* 124, 1841–1857.

Cramer B.D., Schmitz M.D., Huff W.D. & Bergström S.M. 2015: High-precision U–Pb zircon age constraints on the duration of rapid biogeochemical events during the Ludlow Epoch (Silurian Period). *J. Geol. Soc.* 172, 157–160.

Crampton J.S., Cooper R.A., Sadler P.M. & Foote M. 2018: Greenhouse−icehouse transition in the Late Ordovician marks a step change in extinction regime in the marine plankton. *Proceedings of the National Academy of Sciences* 113, 1498–1503.

Dadlez R., Kowalczewski Z. & Znosko J. 1994: Some key problems of the pre-Permian tectonics of Poland. *Geol. Quarterly* 38*,* 169–190.

Fry C.R., Ray D.C., Wheeley J.R., Boomer I., Jarochowska E. & Loydell D.K. 2017: The Homerian carbon isotope excursion (Silurian) within graptolitic successions on the Midland Platform (Avalonia), UK: implications for regional and global comparisons and correlations. *GFF* 139, 301–313.

Frýda J. & Frýdová B. 2014: First evidence for the Homerian (late Wenlock, Silurian) positive carbon isotope excursion from peri-Gondwana: new data from the Barrandian (Perunica). *Bulletin of Geosciences* 89, 617–634.

Frýda J. & Frýdová B. 2016: The Homerian (late Wenlock, Silurian) carbon isotope excursion from Perunica: Does dolomite control the magnitude of the carbon isotope excursion? *Can. J. Earth Sci.* 53, 695–701.

Hammer Ø. & Harper D.A.T. 2008: Paleontological data analysis. *Wiley-Blackwell*, 1–369.

Jaeger H. 1991: Neue Standard-Graptolithenzonenfolge nach der "Grossen Krise" an der Wenlock/Ludlow-Grenze (Silur). *Neues Jahrb. Geol. Paläontol.* 182, 303–354.

Jarochowska E. & Munnecke A. 2016: Late Wenlock carbon isotope excursions and associated conodont fauna in the Podlasie Depression, eastern Poland: a not-so-big crisis? *Geol. J.* 51*,* 683–703.

Jarochowska E., Munnecke A. & Kozłowski W. 2014: An unusual microbial–rostroconch assemblage from the Mulde Event (Homerian, middle Silurian) in Podolia, Western Ukraine. *GFF* 136*,* 120–124.

Jarochowska E., Bremer O., Heidlas D., Pröpster S., Vandenbroucke T.R. & Munnecke A. 2016a: End-Wenlock terminal Mulde carbon isotope excursion in Gotland, Sweden: integration of stratigraphy and taphonomy for correlations across restricted facies and specialized faunas. *Palaeogeogr. Palaeoclimatol. Palaeoecol.* 457*,* 304–322.

Jarochowska E., Munnecke A., Frisch K., Ray D.C. & Castagner A. 2016b: Faunal and facies changes through the mid Homerian (late Wenlock, Silurian) positive carbon isotope excursion in Podolia, western Ukraine. *Lethaia* 49*,* 170–198.

Jarochowska E., Ray D.C., Röstel P., Worton G. & Munnecke A. 2018: Harnessing stratigraphic bias at the section scale: conodont diversity in the Homerian (Silurian) of the Midland Platform, England. *Palaeontology* 61*,* 57–76.

Jeppsson L., Aldridge R. & Dorning K. 1995: Wenlock (Silurian) oceanic episodes and events. *J. Geol. Soc.* 152*,* 487–498.

Kaljo D., Kiipli T. & Martma T. 1997: Carbon isotope event markers through the Wenlock–Pridoli sequence at Ohesaare (Estonia) and Priekule (Latvia). *Palaeogeogr. Palaeoclimatol. Palaeoecol.* 132*,* 211–223.

Kaljo D., Kiipli T. & Martma T. 1998: Correlation of carbon isotope events and environmental cyclicity in the East Baltic Silurian. In: Landing E. & Johnson M.E. (Eds.): Silurian Cycles — Linkages of Dynamic Stratigraphy with Atmospheric, Oceanic and Tectonic Changes. *New York State Museum Bulletin* 491, 297–312.

Kaljo D., Grytsenko V., Martma T. & Mõtus M.A. 2007: Three global carbon isotope shifts in the Silurian of Podolia (Ukraine): stratigraphical implications. *Estonian Journal of Earth Sciences* 56*,* 205–220.

Kiipli T., Radzevičius S., Kallaste T., Motuza V., Jeppsson L. & Wickström L.M. 2008: Wenlock bentonites in Lithuania and correlation with bentonites from sections in Estonia, Sweden and Norway. *GFF* 130*,* 203–210.

Koren' T.N. 1987: Graptolite dynamics in Silurian and Devonian time. *Bulletin of the Geological Society of Denmark* 35*,* 149–160.

Koren' T.N. 1991: The *C. lundgreni* extinction event in Central Asia and its bearing on graptolite biochronology within the Homerian. *Proceedings of the Estonian Academy of Science, Geology* 40*,* 74–78.

Koren' T.N. 1992: New late Wenlock monograptids of the Alai Range. *Paleontologicheskiy Zhumal* 92, 21–33 (in Russian).

Koren' T.N. & Suyarkova A.A. 1994: *Monograptus deubeli* and praedeubeli (Wenlock, Silurian) in the Asian part of the former Soviet Union. *Alcheringa* 18, 85–101

Koren' T.N., Lenz A.C., Loydell D.K., Melchin M.J., Stroch P. & Teller L. 1996: Generalized graptolite zonal sequence defining Silurian time intervals for global paleogeographic studies. *Lethaia* 29*,* 59–60.

Kowalczewski Z., Jaworowski K. & Kuleta M. 1998: Klonów Beds (uppermost Silurian–? lowermost Devonian) and the problem of Caledonian deformations in the Holy Cross Mountains. *Geol. Quarterly* 42*,* 341–378.

Kozłowska A. 2016: A new generic name, *Semigothograptus*, for *Gothograptus? meganassa* Rickards & Palmer, 2002, from the Silurian post-lundgreni Biozone recovery phase, and comparative morphology of retiolitids from the lowermost upper Homerian (upper Wenlock). *Zootaxa* 4208, 534–546.

Kozłowska A., Lenz A. & Melchin M. 2009: Evolution of the retiolitid *Neogothograptus* (Graptolithina) and its new species from the upper Wenlock of Poland, Baltica. *Acta Palaeontologica Polonica* 54*,* 423–434.

Kozłowska-Dawidziuk A., Lenz A.C. & Štorch P. 2001: Upper Wenlock and lower Ludlow (Silurian), post-extinction graptolites, Všeradice section, Barrandian area, Czech Republic. *J. Paleontol.* 75*,* 147–164.

Kozłowski W. 2003: Age, sedimentary environment and palaeogeographical position of the Upper Silurian oolitic beds in the Holy Cross Mountains (Central Poland). *Acta Geologica Polonica* 53*,* 341–357.

Kozłowski W. 2008: Lithostratigraphy and regional significance of the Nowa Słupia Group (Upper Silurian) of the Łysogóry region (Holy Cross Mountains, Central Poland). *Acta Geologica Polonica* 58*,* 43–74.

Kozłowski W. & Munnecke A. 2010: Stable carbon isotope development and sea-level changes during the Late Ludlow (Silurian) of the Łysogóry region (Rzepin section, Holy Cross Mountains, Poland). *Facies* 56*,* 615–633.

Kozłowski W. & Tomczykowa E. 1999: A new occurrence of benthic fauna in the Niewachlów Greywackes (Upper Silurian) from Zalesie near Łagów in the Holy Cross Mountains. *Geol. Quarterly* 43*,* 129–136.

Kozłowski W., Domańska J., Nawrocki J. & Pecskay Z. 2004: The provenance of the Upper Silurian greywackes from the Holy Cross Mountains (Central Poland). *Mineralogical Society of Poland, Special Papers* 24*,* 251–254.

Kozłowski W., Domańska-Siuda J. & Nawrocki J. 2014: Geochemistry and petrology of the Upper Silurian greywackes from the Holy Cross Mountains (central Poland): implications for the Caledonian history of the southern part of the Trans-European Suture Zone (TESZ). *Geol. Quarterly* 58*,* 311–336.

Kozłowski W., Szczepanik Z., Trela W., Zenkner L. & Żylińska A. 2017: Pre-Variscan evolution of the Holy Cross Mountains — Lower Palaeozoic to Middle Devonian. In: Żylińska A. (Ed.): 10th Baltic Stratigraphic Conference, Chęciny 12–14 September 2017. *Abstracts and Guide Book*. Warszawa, 108–136.

Lenz A.C. 1994: Extinction and opportunistic evolution among late Wenlock graptolites. *Lethaia* 27*,* 111–117.

Lenz A.C. 1995: Upper Homerian (Wenlock, Silurian) graptolites and graptolite biostratigraphy, Arctic Archipelago, Canada. *Can. J. Earth Sci.* 32*,* 1378–1392.

Lenz A.C. & Kozłowska A. 2007: Retiolitid diversification and Silurian sea level changes. *Acta Palaeontologica Sinica* 46 (Suppl.), 269–277.

Lenz A.C., Noble P.J., Masiak M., Poulson S.R. & Kozłowska A. 2006: The *lundgreni* Extinction Event: integration of paleontological and geochemical data from Arctic Canada. *GFF* 128*,* 153–158.

Makhnach A.A., Kruchek S.A., Pokrovsky B.G., Strel'tsova G.D., Murashko O.V. & Petrov O.L. 2018: Carbon, oxygen, and sulfur isotope compositions and model of the Silurian rock formation in northwestern Belarus. *Lithology and Mineral Resources* 53*,* 1–13.

Malec J. 2001: Sedimentology of deposits around the Late Caledonian unconformity in the western Holy Cross Mountains. *Geol. Quarterly* 45*,* 397–415.

Maletz J. 2008: Retiolitid graptolites from the collection of Hermann Jaeger in the Museum for Naturkunde, Berlin (Germany). I. *Neogothograptus* and *Holoretiolites*. *Paläontologische Zeitschrift* 82, 285–307.

Maletz J. 2010: Retiolitid graptolites from the collection of Hermann Jaeger II: *Cometograptus*, *Spinograptus* and *Plectograptus*. *Paläontologische Zeitschrift* 84*,* 501–522.

Marshall C., Thomas A.T., Boomer I. & Ray D.C. 2012: High resolution $\delta^{13}C$ stratigraphy of the Homerian (Wenlock) of the English Midlands and Wenlock Edge. *Bulletin of Geosciences* 87*,* 669–679.

Martma T., Brazauskas A., Kaljo D., Kaminskas D. & Musteikis P. 2005: The Wenlock–Ludlow carbon isotope trend in the Vidukle core, Lithuania, and its relations with oceanic events. *Geol. Quarterly* 49*,* 223–234.

Masiak M. 2010: Stop 9. Bardo Prągowiec — Wenlock–Lower Ludlow shales. In: CIMP 2010 Field Trip Guidebook. *Institute of Geological Sciences, Polish Academy of Sciences (PAS),* 51–55.

Melchin M.J., Sadler P.M. & Cramer B.D. 2012: The Silurian Period. In: Gradstein F.M., Ogg J.G., Schmitz M. & Ogg G.M. (Eds.): The Geologic Time Scale 2012, vol. 2. *Elsevier*, 525–558.

Miall A.D. 2010: The geology of stratigraphic sequences (2nd edition). *Springer*, Berlin, 1–522.

Modliński Z. & Szymański B. 2001: The Silurian of the Nida, Holy Cross Mts. and Radom areas, Poland — a review. *Geol. Quarterly* 45*,* 435–454.

Narkiewicz M. 2002: Ordovician through earliest Devonian development of the Holy Cross Mts. (Poland): Constraints from subsidence analysis and thermal maturity data. *Geol. Quarterly* 46*,* 255–266.

Nawrocki J., Dunlap J., Pecskay Z., Krzemiński L., Żylińska A., Fanning M., Kozłowski W., Salwa S., Szczepanik Z. & Trela W. 2007: Late Neoproterozoic to Early Palaeozoic palaeogeography of the Holy Cross Mountains (Central Poland): an integrated approach. *J. Geol. Soc., London* 164*,* 405–423.

Nawrocki J., Salwa S. & Pańczyk M. 2013: New ^{40}Ar–^{39}Ar age constraints for magmatic and hydrothermal activity in the Holy Cross Mts. (southern Poland). *Geol. Quarterly* 57*,* 551–560.

Noble P.J., Zimmerman M.K., Holmden C. & Lenz A.C. 2005: Early Silurian (Wenlockian) $\delta^{13}C$ profiles from the Cape Phillips Formation, Arctic Canada and their relation to biotic events. *Can. J. Earth Sci.* 42*,* 1419–1430.

Oksanen J., Blanchet F.G., Friendly M., Kindt R., Legendre P., McGlinn D., Minchin P.R., O'Hara R.B., Simpson G.L., Solymos P., Stevens M.H.H., Szoecs E. & Wagner H. 2018: Package 'vegan'. Community ecology package. https://cran.r-project.org/package=vegan.

Paškevičius J., Lapinskas P., BrazauskasA., Musteikis P. & Jacyna J. 1994: Stratigraphic revision of the regional stages of the Upper Silurian part in the Baltic Basin. *Geologija* (Vilnius) 17*,* 64–87.

Patzkowsky M.E. & Holland S.M. 2012: Stratigraphic paleobiology: understanding the distribution of fossil taxa in time and space. *University of Chicago Press*, 1–256.

Peters S.E. & Foote M. 2002: Determinants of extinction in the fossil record. *Nature* 416, 6879, 420.

Porębska E., Kozłowska–Dawidziuk A. & Masiak M. 2004: The *lundgreni* event in the Silurian of the East European platform, Poland. *Palaeogeogr. Palaeoclimatol. Palaeoecol.* 213*,* 271–294.

R Development Core Team 2015: R: A Language and Environment for Statistical Computing. Version 3.1.3. *R Foundation for Statistical Computing*, Vienna. https://www.r-project.org/.

Radzevičius S. 2006: Late Wenlock biostratigraphy and the *Pristiograptus virbalensis* group (Graptolithina) in Lithuania and the Holy Cross Mountains. *Geol. Quarterly* 50*,* 333–344.

Radzevičius S. & Paškevičius J. 2005: *Pristiograptus* (Graptoloidea) from the Upper Wenlock of the Baltic Countries. *Stratigraphy and Geological Correlation* 13*,* 159–169.

Radzevičius S., Spiridonov A. & Brazauskas A. 2014a: Integrated middle–upper Homerian (Silurian) stratigraphy of the Viduklė-61 well, Lithuania. *GFF* 136*,* 218–222.

Radzevičius S., Spiridonov A. & Brazauskas A. 2014b: Application of Wavelets to the Cyclostratigraphy of the Upper Homerian (Silurian) Gėluva Regional Stage in the Viduklė-61 Deep Well (Western Lithuania). In: Rocha R., Pais J., Kullberg J.C. & Finney S. (Eds.): STRATI 2013. First International Congress on Stratigraphy. At the Cutting Edge of Stratigraphy. *Springer*, 437–440.

Radzevičius S., Spiridonov A., Brazauskas A., Norkus A., Meidla T. & Ainsaar L. 2014c: Upper Wenlock $\delta^{13}C$ chemostratigraphy, conodont biostratigraphy and palaeoecological dynamics in the Ledai-179 drill core (Eastern Lithuania). *Estonian Journal of Earth Sciences* 63*,* 293–299.

Radzevičius S., Spiridonov A., Brazauskas A., Dankina D., Rimkus A., Bičkauskas G., Kaminskas D., Meidla T. & Ainsaar L. 2016: Integrated stratigraphy, conodont turnover and palaeoenvironments of the upper Wenlock and Ludlow in the shallow marine succession of the Vilkaviškis-134 core (Lithuania). *Newsletters on Stratigraphy* 49*,* 321–336.

Radzevičius S., Tumakovaitė B. & Spiridonov A. 2017: Upper Homerian (Silurian) high-resolution correlation using cyclostratigraphy: an example from western Lithuania. *Acta Geologica Polonica* 67*,* 307–322.

Raup D.M. & Crick R.E. 1979: Measurement of faunal similarity in paleontology. *J. Paleontol.* 53*,* 1213–1227.

Rickards R.B. & Palmer D.C. 2002: *Gothograptus*? *meganassa* sp. nov., an unusually large retiolitid graptoloid from the Late Wenlock ludensis Biozone of Long Mountain, Shropshire, UK. *Special Papers in Palaeontology* 67, 225–232.

Ryka W. & Tomczyk H. 1959: Bentonites in old Palaeozoic sediments from the Holy Cross Mountains. *Geol. Quarterly* 3*,* 710–712 (in Polish with English summary).

Saltzman M.R. 2001: Silurian $\delta^{13}C$ stratigraphy: a view from North America. *Geology* 29*,* 671–674.

Samtleben C., Munnecke A., Bickert T. & Pätzold J. 1996: The Silurian of Gotland (Sweden): facies interpretation based on stable isotopes in brachiopod shells. *Geologische Rundschau* 85*,* 278–292.

Samtleben C., Munnecke A. & Bickert T. 2000: Development of facies and C/O-isotopes in transects through the Ludlow of Gotland: evidence for global and local influences on a shallow-marine environment. *Facies* 43*,* 1–38.

Shebolkin D.N. & Männik P. 2014: Wenlock strata in the southern part of the Chernyshev Ridge (Timan–northern Ural region). *Litosfera/Lithosphere* 1*,* 33−40.

Spiridonov A. 2017: Recurrence and cross recurrence plots reveal the onset of the Mulde event (Silurian) in the abundance data for Baltic conodonts. *The Journal of Geology* 125*,* 381–398.

Spiridonov A., Brazauskas A. & Radzevičius S. 2016: Dynamics of abundance of the mid-to late Pridoli conodonts from the Eastern part of the Silurian Baltic Basin: multifractals, state shifts, and oscillations. *Am. J. Sci.* 316, 4,363–400.

Spiridonov A., Kaminskas D., Brazauskas A. & Radzevičius S. 2017a: Time hierarchical analysis of the conodont paleocommunities and environmental change before and during the onset of the lower Silurian Mulde bioevent–A preliminary report. *Global Planet. Change* 157*,* 153–164.

Spiridonov A., Venckutė-Aleksienė A. & Radzevičius S. 2017b: Cyst size trends in the genus *Leiosphaeridia* across the Mulde (lower Silurian) biogeochemical event. *Bulletin of Geosciences* 92, 391–404.

Štorch P. 1994: Graptolite biostratigraphy of the Lower Silurian (Llandovery and Wenlock) of Bohemia. *Geol. J.* 29*,* 137–165.

Štorch P., Manda Š. & Loydell D.K. 2014: The early Ludfordian *leintwardinensis* graptolite event and the Gorstian–Ludfordian boundary in Bohemia (Silurian, Czech Republic). *Palaeontology* 57*,* 1003–1043.

Štorch P., Manda Š., Slavík L. & Tasáryová Z. 2016: Wenlock–Ludlow boundary interval revisited: New insights from the off-shore facies of the Prague Synform, Czech Republic. *Can. J. Earth Sci.* 53*,* 666–673.

Sullivan N.B., McLaughlin P.I., Emsbo P., Barrick J.E. & Premo W.R. 2016: Identification of the late Homerian Mulde Excursion at the base of the Salina Group (Michigan Basin, USA). *Lethaia* 49*,* 591–603.

Sullivan N.B., Loydell D.K., Montgomery P., Molyneux S.G., Zalasiewicz J., Ratcliffe K.T. & Lewis G. 2018: A record of Late Ordovician to Silurian oceanographic events on the margin of Baltica based on new carbon isotope data, elemental geochemistry, and biostratigraphy from two boreholes in central Poland. *Palaeogeogr. Palaeoclimatol. Palaeoecol.* 490*,* 95–106.

Tomczyk H. 1958: The lower Ludlovian in a bore-hole at Mędrzechów near Tarnów (Subcarpatians) (Preliminary Report). *Geol. Quarterly* 2*,* 311–320 (in Polish with English summary).

Tomczyk H. 1962: Stratigraphic problems of the Ordovician and Silurian in Poland in the light of recent studies. *Prace Instytutu Geologicznego* 35*,* 1–134 (in Polish with English summary).

Tomczykowa E. 1957: Trilobites from Wenlock and Lower Ludlow graptolitic shales of the Swięty Krzyż Mountains. *Prace Instytutu Geologicznego* 122*,* 83–114 (in Polish with English summary).

Tomczykowa E. 1993: Upper Ludlow trilobites from the southern part of the Holy Cross Mts. *Geol. Quarterly* 37*,* 359–384.

Ulst R. 1974: The early sequence of pristiograptids in conterminous deposits of Wenlock and Ludlow of the Middle Prebaltic. In: Obut A. (Ed.): Graptolity SSSR. *Nauka*, 90–105 (in Russian).

Urbanek A., Radzevičius S., Kozłowska A. & Teller L. 2012: Phyletic evolution and iterative speciation in the persistent *Pristiograptus dubius* lineage. *Acta Palaeontologica Polonica* 57, 589–611.

Vecoli M., Riboulleau A. & Versteegh G.J.M. 2009: Palynology, organic geochemistry and carbon isotope analysis of a latest Ordovician through Silurian clastic succession from borehole Tt1, Ghadamis Basin, southern Tunisia, North Africa: palaeoenvironmental interpretation. *Palaeogeogr. Palaeoclimatol. Palaeoecol.* 273*,* 378–394.

Venckutė-Aleksienė A., Radzevičius S. & Spiridonov A. 2016: Dynamics of phytoplankton in relation to the upper Homerian (Lower Silurian) lundgreni event — An example from the Eastern Baltic Basin (Western Lithuania). *Mar. Micropaleont.* 126*,* 31–41.

Wenzel B. & Joachimski M.M. 1996: Carbon and oxygen isotopic composition of Silurian brachiopods (Gotland/Sweden): palaeoceanographic implications. *Palaeogeogr. Palaeoclimatol. Palaeoecol.* 122*,* 143–166.

Walczak A. & Belka Z. 2017: Fingerprinting Gondwana versus Baltica provenance: Nd and Sr isotopes in Lower Paleozoic clastic rocks of the Małopolska and Łysogóry terranes, southern Poland. *Gondwana Res.* 45*,* 138–151.

Zalasiewicz J.A. & Williams M. 1999: Graptolite biozonation of the Wenlock (Silurian) rocks of the Builth Wells district, central Wales. *Geol. Mag.* 136*,* 263–283

Zalasiewicz J.A., Taylor L., Rushton A.W.A., Loydell D.K., Rickards R.B. & Williams M. 2009: Graptolites in British stratigraphy. *Geol. Mag.* 146*,* 785–850.

Appendix

Graptolite data used in multivariate analysis

Zone/taxon	*P. ludensis*	*P. frequens*	*C. gerhardi*	*P. virbalensis*	*C. deubeli*	*Gothograptus* sp.	*P. praedeubeli*
praedeubeli	0	0	0	1	0	0	0
praedeubeli	0	0	0	1	0	0	1
praedeubeli	0	0	0	0	0	0	1
praedeubeli	0	0	0	0	0	0	1
praedeubeli	0	0	0	1	0	0	1
praedeubeli	0	0	0	1	0	0	1
praedeubeli	0	0	0	1	0	0	0
praedeubeli	0	0	0	0	0	0	1
praedeubeli	0	0	0	0	0	0	1
praedeubeli	0	0	0	0	0	0	1
praedeubeli	0	1	0	1	0	1	1
praedeubeli	0	0	0	0	0	0	1
praedeubeli	0	0	0	0	0	0	1
praedeubeli	0	0	0	0	0	0	1
praedeubeli	0	0	0	0	0	1	1
deubeli	0	0	0	0	1	1	0
deubeli	0	0	0	0	1	0	0
deubeli	0	0	0	0	1	1	0
deubeli	0	0	0	0	1	0	0
deubeli	0	0	0	0	1	0	1
deubeli	0	1	0	0	1	0	1
deubeli	0	0	0	0	1	0	0
deubeli	0	0	0	1	1	0	0
deubeli	0	0	0	0	1	0	1
deubeli	0	0	0	0	1	0	0
deubeli	0	0	0	0	1	0	0
deubeli	0	0	0	0	1	1	1
ludensis	1	1	0	0	0	0	0
ludensis	0	1	1	0	0	0	0
ludensis	1	0	0	0	0	0	0
ludensis	0	0	1	0	0	0	0
ludensis	0	0	1	0	0	0	0
ludensis	1	1	0	0	0	0	0
ludensis	1	0	0	1	0	0	0
ludensis	1	1	0	1	0	0	0
ludensis	1	1	0	0	0	0	0
ludensis	1	0	0	0	0	0	0
ludensis	1	0	0	0	0	0	0
ludensis	1	0	0	0	0	0	0
ludensis	1	0	0	0	0	0	0
ludensis	1	0	1	1	0	0	0
ludensis	1	1	0	0	0	0	0
ludensis	1	0	0	1	0	0	0
ludensis	1	1	0	0	0	0	0
ludensis	1	0	0	1	0	0	0